# Analytical method for establishing indentation rolling resistance

*Lech* Gładysiewicz[1], and *Martyna* Konieczna[1,*]

[1]Wroclaw University of Science and Technology, Faculty of Geoengineering, Mining and Geology, 27 Wyb. Wyspianskiego St., 50-370 Wroclaw, Poland

**Abstract.** Belt conveyors are highly reliable machines able to work in special operating conditions. Harsh environment, long distance of transporting and great mass of transported martials are cause of high energy usage. That is why research in the field of belt conveyor transportation nowadays focuses on reducing the power consumption without lowering their efficiency. In this paper, previous methods for testing rolling resistance are described, and new method designed by authors was presented. New method of testing rolling resistance is quite simple and inexpensive. Moreover it allows to conduct the experimental tests of the impact of different parameters on the value of indentation rolling resistance such as core design, cover thickness, ambient temperature, idler travel frequency, or load value as well. Finally results of tests of relationship between rolling resistance and idler travel frequency and between rolling resistance and idler travel speed was presented.

## 1 Introduction

Belt conveyors are vital elements of transportation systems in both underground and surface mines, as well as in many other branches of industry. They allow the most economical and, frequently, also the fastest transportation of materials. Nevertheless, the maintenance of belt conveyors generates significant costs. Conveyor belt has two important functions in the operation of a belt conveyor – it transports the bulk materials and transmits the driving force; at the same time, however, it generates different types of resistances. Rational belt management must be based on the knowledge of the phenomena that occur during the operation of a belt conveyor. Expanding this knowledge requires increasingly precise tests [1-3] and theoretical analyses, which allow the description and prediction of how a belt will behave in given operating conditions [4- 6]. From the perspective of energy losses, the rolling resistances of the belt on idlers constitute the most significant component of the resistances observed on a belt conveyor. Precise calculation of belt damping factor proves crucial if the theoretically established values of resistances are to correspond to the values established experimentally.

* Corresponding author: martyna.konieczna@pwr.edu.pl

© The Authors, published by EDP Sciences. This is an open access article distributed under the terms of the Creative Commons Attribution License 4.0 (http://creativecommons.org/licenses/by/4.0/).

Symbols:

$\varphi_1$, $\varphi_2$ - entry angle and exit angle of the belt on the idler, radians
$\sigma$ - compressive stresses acting on the belt, Pa
$\xi$ - measure of belt damping expressed as the ratio of $\varphi_2$ and $\varphi_1$, -
$\psi$ - belt damping factor expressed through $\delta$, -
$t_0$ - duration of a single load cycle, s
$t_m$ - time to maximum transverse strain of the belt,
$\omega_0$ - angular velocity of the idler, $\frac{rad}{s}$
$v_t$ - belt speed, $\frac{m}{s}$
$\delta$ - phase lag angle, radians
$\varepsilon$ - transverse strains, -
$\varepsilon_1$ - particular solution (viscous flow), -
$\varepsilon_2$ - general solution (typical for harmonic load), -
$\tau_0$ - time constant of the belt's model, -
$D_k$ - idler diameter, m
$E_c$ - modulus of elasticity / resultant modulus of the belt under transverse compression (allowing for a number of plies in the belt), Pa
$h_0$ - active belt thickness undergoing the process of compression, m
$F$ - belt damping function, -
$e_1$ - unit elastic energy transferred to belt, J
$e_2$ - recovered energy, J

## 2 Rolling resistances of the belt on idlers

Various forms of energy conversions occur during the operation of a belt conveyor. These conversions generate a variety of resistances. The motion resistances of a belt conveyor, as classified by their location, include [7]:

- concentrated resistances (on the head pulley, drive pulley, tail pulley and take-up pulley)
- main resistances (distributed along the whole conveyor route),
- lift resistances of the belt and of the bulk material (on the inclined sections of the conveyor route).

For conveyor belts longer than 80 m, main resistances are the dominant component of motion resistance. Depending on how energy is dissipated, main resistances are classified as follows [7]:

- idler rotational resistance $W_k$,
- rolling resistance of belt on idlers $W_e$,
- belt flexure resistance $W_b$,
- flexure resistance of bulk material $W_f$,
- sliding resistance of belt on idlers $W_r$.

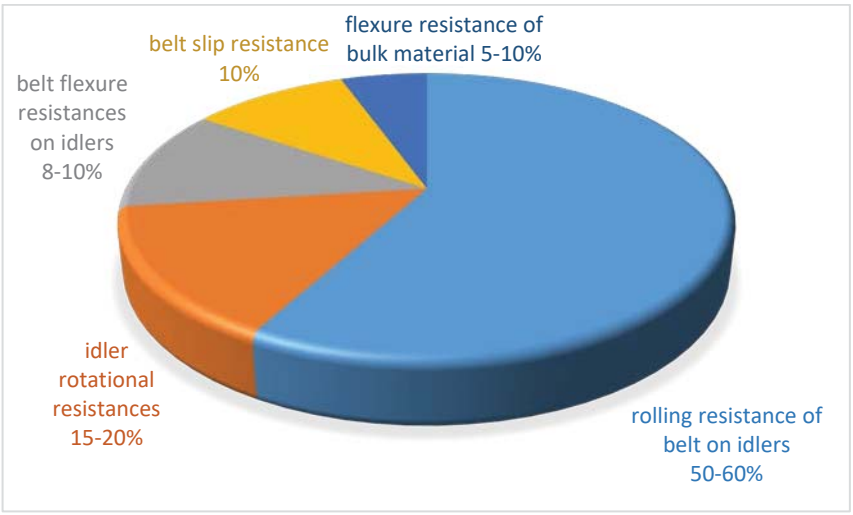


**Fig. 1.** Approximate values of the components of main resistances on a belt conveyor for the belt's top run [7].

Indentation rolling resistances, also referred to as belt indentation resistances, are the main component of motion resistances which occur on a conveyor. They may account for as much as 60% of the total resistance to motion, and consequently they also generate the greatest energy losses.

**Tab. 1.** Estimation of savings resultant from limiting belt conveyor resistance to motion in a mine, which operates approx. 100 km of conveyors [8].

| **Decrease in resistances [%]** | **5** | **10** | **15** | **20** | **25** | **30** |
|---|---|---|---|---|---|---|
| **Savings** $\left[\frac{million\ pln}{year}\right]$ | 4.69 | 9.38 | 14.06 | 18.75 | 23.44 | 28.13 |

Estimation of savings presented in tab. 1 reveals how even small decrease in resistances of conveyors can be profitable. Resistances reduction of 5% equal more than 4.5 million pln. The precise calculations of indentation rolling resistance will enable to determine the energy consumption more correctly.

## 3 Theoretical belt damping factor

Belt load on a single idler set is accompanied by temporary strain in belt. Due to the belt's viscoelastic properties, the strain occurs not only in the contact zone of the belt and the idler, but also outside this zone. Therefore, the load-strain relationship is not linear, and the belt resumes its initial state with some delay; this phenomenon is referred to as viscous flow [9, 10] Figure 2 shows the relationship between harmonic load and strain in subsequent cycles.

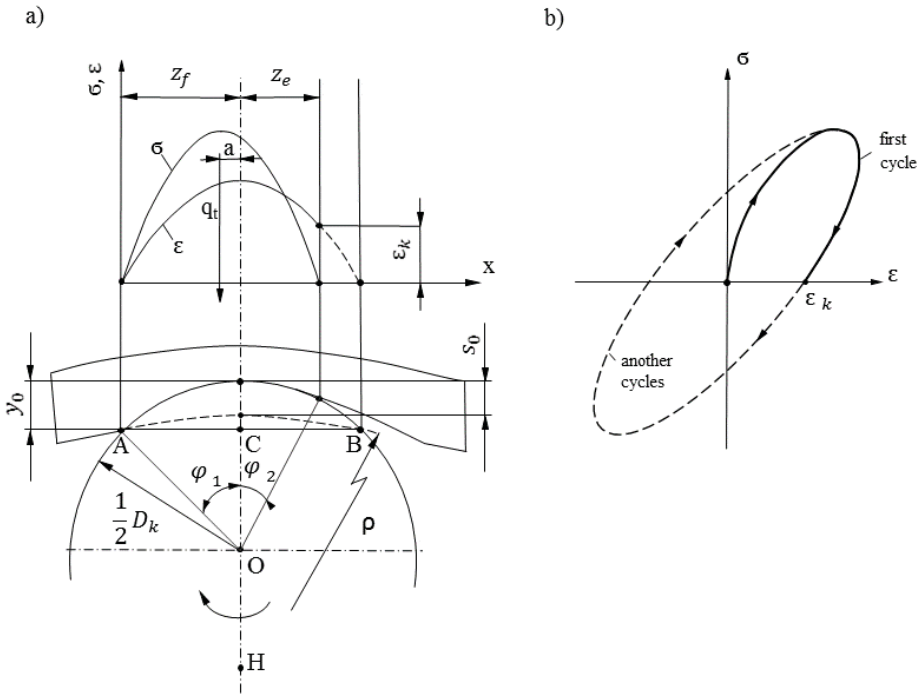


**Fig. 2.** a) stress and strain distribution in contact zone between belt and idler set, b) deformations in a viscoelastic belt and hysteresis loop for the first and for the consecutive stress cycles [4].

When moving on the supporting idlers, a conveyor belt is subjected to a momentary indentation due to external forces. As the distances between idler sets on an actual belt conveyor are large, before each cycle starts, the belt resumes its initial state. Therefore, the theoretical model was developed on the basis of a hysteresis loop which corresponds to the first stress cycle. The compressive stress curve is a harmonic function, which may be expressed with a simple formula:

$$\sigma = \sigma_0 \cdot \sin(\omega_0 \cdot t) \tag{1}$$

For the belt's model, the formula is as follows:

$$\sigma = E_c \cdot \left( \varepsilon + \tau_0 \cdot \frac{d\varepsilon}{dt} \right) \tag{2}$$

Strain in conveyor belts has two components: a general and a particular solution of the belt equation. The general solution is described by the following equation:

$$\varepsilon_1 = \frac{\sigma_0}{E_c} \cdot \cos\delta \cdot \sin\delta \cdot e^{-\frac{t}{\tau_0}} \tag{3}$$

The particular solution is as follows:

$$\varepsilon_2 = \frac{\sigma_0}{E_c} \cdot \cos\delta \cdot \sin\left(\omega_0 \cdot t - \delta\right) \tag{4}$$

The duration of a single load cycle is:

$$t_0 = \frac{D_K}{2 \cdot v_t} \cdot \left(\varphi_1 + \varphi_2\right) \tag{5}$$

Whereas the time to maximum transverse strain of the belt is described by the following formula:

$$t_m = \frac{D_K}{2 \cdot v_t} \cdot \varphi_1 = \frac{t_0}{1+\xi} \tag{6}$$

Unit strain energy of the belt may be expressed with the following equation:

$$de = \sigma \cdot h_0 \cdot d\varepsilon = \sigma \cdot h_0 \cdot \left(d\varepsilon_1 + d\varepsilon_2\right) \tag{7}$$

$$d\varepsilon_1 = -\frac{\sigma_0}{E_c \cdot \tau_0} \cdot \sin\delta \cdot \cos\delta \cdot e^{-\frac{t}{\tau_0}} \cdot dt \tag{8}$$

$$d\varepsilon_2 = \frac{\sigma_0}{E_c \cdot \tau_0} \cdot \omega_0 \cdot \cos\delta \cdot \cos\left(\omega_0 \cdot t - \delta\right) \cdot dt \tag{9}$$

During the time between $t$=0 and $t$=$t_m$, energy $e_1$ is transferred to the belt, while during the time between $t$=$t_m$ and $t$=$t_0$, only part of this energy $e_2$ is recovered. Thus, the belt's damping factor, which depends on the energy lost and on the energy transferred to the belt in a single compression cycle, is described by the following formula:

$$\psi_{th} = \frac{\int_0^{t_0} \sigma(t) \cdot d\varepsilon}{\int_0^{t_m} \sigma(t) \cdot d\varepsilon} \tag{10}$$

Unit elastic energy converted (lost) in a single compression cycle is:

$$e_1 = h_0 \cdot \int_0^{t_0} \sigma(t) \cdot d\varepsilon = \frac{h_0 \cdot \sigma_0^2}{E_c} \cdot \cos\beta_z \cdot \int_0^{t_0} \left[ -\frac{\sin\delta}{\tau_0} \cdot \sin\left(\omega_0 \cdot t\right) \cdot e^{-\frac{t}{\tau_0}} + \omega_0 \cdot \sin\left(\omega_0 \cdot t\right) \cdot \cos\left(\omega_0 \cdot t - \delta\right) \right] \cdot dt \tag{11}$$

Elastic energy transferred to the belt in a single compression cycle is:

$$e_2 = h_0 \cdot \int_0^{t_m} \sigma(t) \cdot d\varepsilon = \frac{h_0 \cdot \sigma_0^2}{E_c} \cdot \cos\beta_z \cdot \int_0^{t_m} \left[ -\frac{\sin\delta}{\tau_0} \cdot \sin\left(\omega_0 \cdot t\right) \cdot e^{-\frac{t}{\tau_0}} + \omega_0 \cdot \sin\left(\omega_0 \cdot t\right) \cdot \cos\left(\omega_0 \cdot t - \delta\right) \right] \cdot dt \tag{12}$$

The calculations are based on the following assumptions:

$$\omega_0 \cdot \tau_0 = tg\delta \tag{13}$$

$$\frac{\sin\delta}{\omega_0^2 \cdot \tau_0^2 + 1} = \cos^2\delta \cdot \sin\delta \tag{14}$$

$$\omega_0 \cdot t_0 = \pi \tag{15}$$

$$\omega_0 \cdot t_m = \frac{\pi}{1+\xi} \tag{16}$$

$$-\frac{t_m}{\tau_0} = -\frac{\pi}{(1+\xi)\cdot tg\delta} \tag{17}$$

$$-\frac{t_0}{\tau_0} = -\frac{\pi}{tg\delta} \tag{18}$$

$$\delta_z = \frac{\pi}{2} \cdot \frac{1-\xi}{1+\xi} \tag{19}$$

$$\omega_0 = \frac{2\cdot\pi\cdot v_t}{D_K \cdot (\varphi_1 + \varphi_2)} = \frac{2\cdot\pi\cdot v_t}{D_K \cdot \varphi_1 \cdot (1+\xi)} \tag{20}$$

The final shapes for the $e_1$ and $e_2$ equations are as follows:

$$e_1 = \frac{h_0\cdot\sigma_0^2}{E_c} \cdot cos\left(\frac{\pi}{2}\cdot\frac{1-\xi}{1+\xi}\right) \cdot \left\{ e^{-\frac{\pi}{tg\left(\frac{\pi}{2}\frac{1-\xi}{1+\xi}\right)}} \cdot cos^2 \cdot \left(\frac{\pi}{2}\cdot\frac{1-\xi}{1+\xi}\right) \cdot \sin\left(\frac{\pi}{2}\cdot\frac{1-\xi}{1+\xi}\right) \cdot (-\pi) + \frac{\pi\cdot sin\left(\frac{\pi}{2}\frac{1-\xi}{1+\xi}\right)}{2} \right\} \tag{11'}$$

$$e_2 = \frac{h_0\cdot\sigma_0^2}{E_c} \cdot cos\left(\frac{\pi}{2}\cdot\frac{1-\xi}{1+\xi}\right) \cdot \left\{ e^{-\frac{\pi}{(1+\xi)\cdot tg\left(\frac{\pi}{2}\frac{1-\xi}{1+\xi}\right)}} \cdot cos^2 \cdot \left(\frac{\pi}{2}\cdot\frac{1-\xi}{1+\xi}\right) \cdot \sin\left(\frac{\pi}{2}\cdot\frac{1-\xi}{1+\xi}\right) \cdot \left[ \frac{\pi}{1+\xi} \cdot cos\left(\frac{\pi}{1+\xi}\right) + sin\left(\frac{\pi}{1+\xi}\right) \right] + \frac{\frac{2\pi}{1+\xi}\cdot\sin\left(\frac{\pi}{1+\xi}\right) - cos\left(\frac{2\pi}{1+\xi} - \frac{\pi}{2}, \frac{1-\xi}{1+\xi}\right)}{4} + \frac{cos\left(-\frac{\pi}{2}\frac{1-\xi}{1+\xi}\right)}{4} \right\} \tag{12'}$$

After reduction, the measure for belt damping is expressed as the relationship between the energy lost and the energy transferred to the belt:

$$\psi_{th} = \frac{e_1}{e_2} \tag{21}$$

Thus, the formula for damping factor in function of phase lag angle is as follows:

$$\psi(\delta)_{th} = \frac{e^{-\frac{\pi}{tg\delta}\cdot cos^2\delta\cdot(-\pi)+\frac{\pi}{2}}}{e^{\frac{-\frac{\pi}{2}+\delta}{tg\delta}\cdot cos^2\cdot\left[-\left(\frac{\pi}{2}+\delta\right)\cdot sin\delta + cos\delta\right] + \left(\frac{\frac{\pi}{2}+\delta+ctg\delta}{2}\right)}} \tag{22}$$

## 4 Damping factor determined in laboratory tests

The hysteresis loop, which is the result of cyclic compression, shows the belt's load-strain relationship. The damping factor may be expressed as the relationship between the area inside the hysteresis loop (converted energy) and the area below the load curve (delivered energy). The belt's modulus of elasticity may be calculated as the inclination angle of the straight line which connects the vertices of the loop. These values are calculated on the basis of the hysteresis loop established in laboratory tests. The belt's hysteresis loop which would be adequate to the belt's cyclic indentation process is not obtainable in laboratory conditions. Therefore, a loop recorded during continuous harmonic load is used (Figure 2). In the case of laboratory tests, the course of compressive stresses may be expressed with the following formula:

$$\sigma = \sigma_0 + \sigma_0 \cdot \sin(\omega \cdot t) \tag{23}$$

Solution of the belt's differential equation:

$$\varepsilon = \varepsilon_0 + \frac{\sigma_0}{E_C} \cdot cos\delta \cdot \sin(\omega_0 \cdot t - \delta) \tag{24}$$

$$d\varepsilon = \frac{\sigma_0}{E_C} \cdot cos\delta \cdot \omega_0 \cdot \cos(\omega_0 t - \delta) dt \tag{25}$$

$$\sigma = \sigma_0 + \sigma_0 \cdot \sin\alpha \tag{26}$$

$$\varepsilon = \varepsilon_0 + \frac{\sigma_0}{E_C} \cdot cos\delta \cdot \sin(\alpha - \delta) \tag{27}$$

$$d\varepsilon = \frac{\sigma_0}{E_C} \cdot cos\delta \cdot \omega_0 \cdot \cos(\alpha - \delta) d\alpha \tag{28}$$

$$de = \sigma \cdot h_0 \cdot d\varepsilon \tag{29}$$

$$de = h_0 \cdot (\sigma_0 + \sigma_0 \cdot sin\alpha) \cdot \frac{\sigma_0}{E_C} \cdot cos\delta \cdot \cos(\alpha - \delta)\, d\alpha \tag{30}$$

$$de = \frac{h_0 \cdot \sigma_0^2}{E_C} \cdot cos\delta \cdot [cos(\alpha - \delta) + sin\alpha \cdot cos(\alpha - \delta)] d\alpha \tag{31}$$

Unit elastic energy lost in a single compression cycle in laboratory conditions is:

$$e_1 = \frac{h_0 \cdot \sigma_0^2}{E_C} \cdot cos\delta \cdot \left[\int_0^{2\pi} \cos(\alpha - \delta)\, d\alpha + \int_0^{2\pi} sin\alpha \cdot \cos(\alpha - \delta) d\alpha\right] \tag{31}$$

Where:

$$\int_0^{2\pi} \cos(\alpha - \delta)\, d\alpha = 0, \qquad and \int_0^{2\pi} sin\alpha \cdot \cos(\alpha - \delta) d\alpha = \pi \cdot sin\delta$$

$$e_1 = \frac{h_0 \cdot \sigma_0^2}{E_C} \cdot cos\delta \cdot \pi \cdot sin\delta \tag{32}$$

Elastic energy transferred to the belt in a single compression cycle is:

$$e_2 = \frac{h_0 \cdot \sigma_0^2}{E_C} \cdot cos\delta \cdot \left[\int_{\frac{3}{2}\pi+\delta}^{\frac{5}{2}\pi+\delta} cos(\alpha - \delta) d\alpha + \int_{\frac{3}{2}\pi+\delta}^{\frac{5}{2}\pi+\delta} sin\delta \cdot \cos(\alpha - \delta) d\alpha\right] \tag{33}$$

$$e_2 = \frac{h_0 \cdot \sigma_0^2}{E_C} \cdot cos\delta \cdot \left[\frac{1}{2} \cdot \pi \cdot sin\delta + 2\right] \tag{34}$$

The above served to describe the damping factor established in laboratory tests:

$$\psi_{lab} = \frac{e_1}{e_2} \tag{35}$$

$$\psi_{lab} = \frac{\pi \cdot sin\delta}{\frac{\pi}{2} sin\delta + 2} \tag{36}$$

## 5 Comparison of the theoretical model with the results of laboratory tests

Below are presented two hysteresis loop. First (fig. 3a) in adequate for the theoretical model and describes only the first cycle of loading. The next one has schematic shape of loop established in laboratory tests. To obtain the regular loop it is necessary to start the measurement with load. That is why the laboratory loop is transferred in comparison to the theoretical loop.

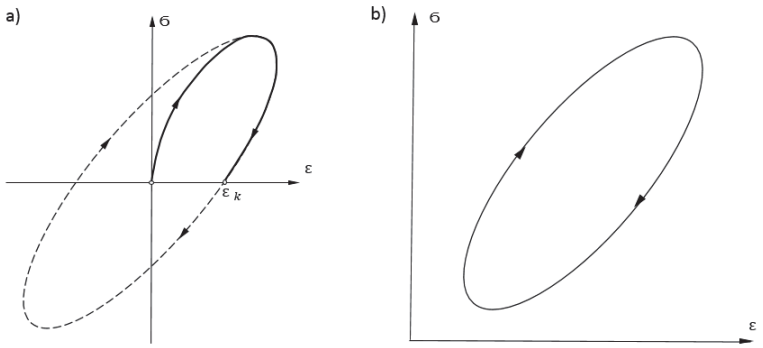


**Fig. 3.** Hysteresis loop: a) for the theoretical model b) schematic shape of loop adequate for laboratory tests [11].

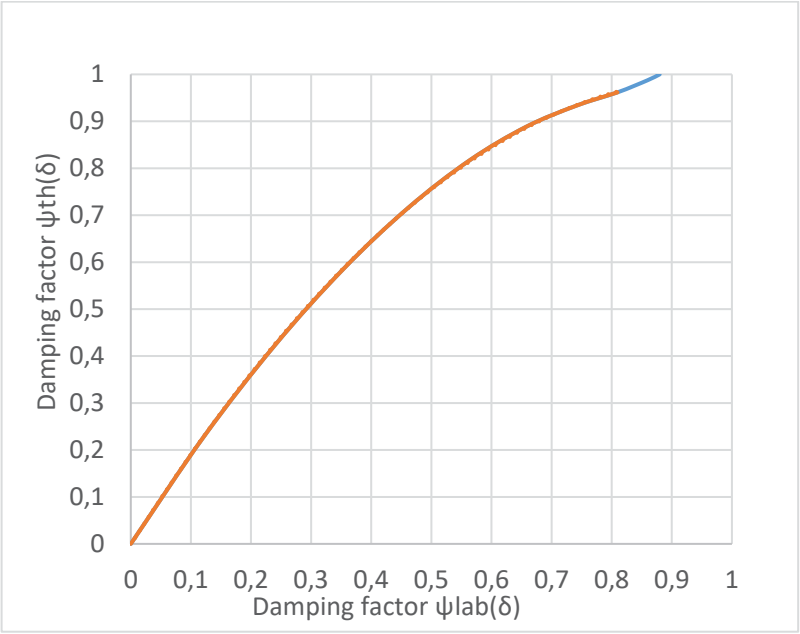


**Fig. 4.** Relationship between the damping factor established theoretically and in laboratory tests [11].

An equation describing the relationship between the damping factor as calculated theoretically and as found in laboratory tests:

$$\psi_{th} = -1.0385\psi_{lab}^2 + 2.0334\psi_{lab} - 0.0021 \quad (37)$$

The origin of the above diagram (in point 0,0) is purely hypothetical, since damping does not occur then, and this is an abstract situation in the case of a conveyor belt. Equation (37) describes the curve until damping factor 0.8 is reached. The part of the curve which is designated with blue color was not included in the following analyses, since values above 0.8 are practically unobtainable and only introduce disturbance to the characteristic curve. Equation (37) may serve to draw an analytical relationship between the rolling resistance based on the laboratory-determined damping factor and the rolling resistance determined for a conveyor belt operated in actual mining conditions.

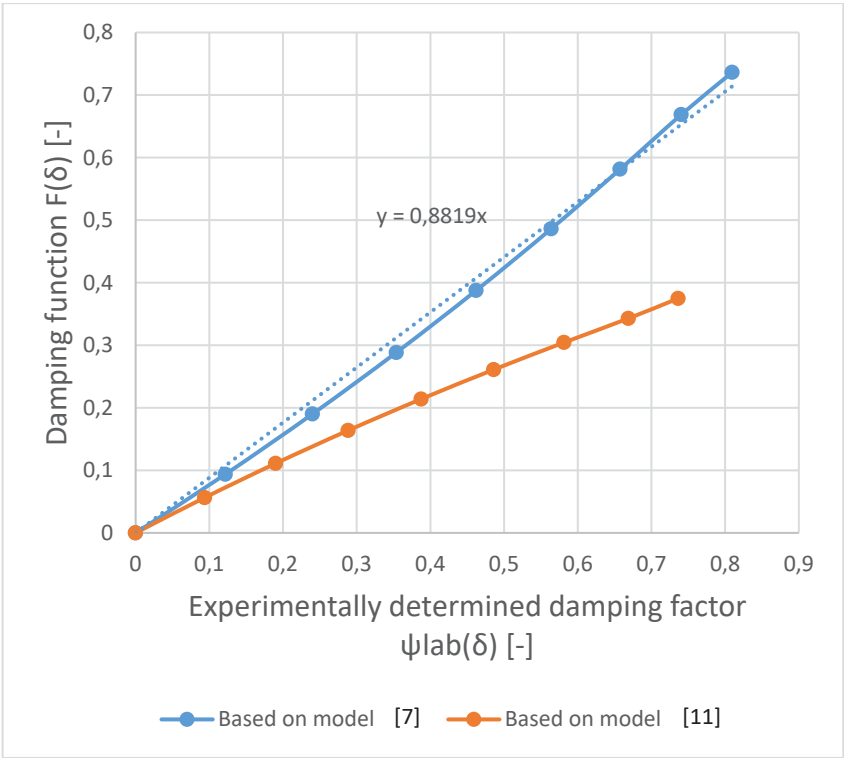


**Fig. 5.** Relationship between the damping function and the experimentally determined damping factor.

Regardless of the model used [7, 11], if it is bi-parameter, the rolling resistances are calculated from the relationship between the product of the damping factor and the structural parameters [7]. Comparison of different conveyor belts is based on an assumption that they are used similarly and that they work in identical conditions. In such case, damping function *F* is sufficient for analysis. In the diagram above, damping function is compared with laboratory damping factor. As can be observed, the convergence between the damping function and the experimental damping factor approaches 90% (0.8819). Moreover, the values are convergent regardless of the value of rolling resistance. The convergence is fixed for both low and high rolling resistances. The previously determined coefficient of convergence between the two values was lower: 0.463 [11]. Defining more precise

assumptions for the model allowed improving the coefficient almost twice [7], and thus allowed approximating the theoretically calculated values of rolling resistances to the values measured in the laboratory.

$$w_e = F \cdot \sqrt[3]{\frac{q_T^4}{D_K^2 \cdot \lambda \cdot c_e}} \tag{38}$$

$$F(\xi) = \sqrt[3]{\frac{\pi \cdot (1-\xi)^3}{2 \cdot (\xi+1)} \cdot \left\{ \frac{1}{2} \cdot \sin\left( \pi \cdot \frac{1-\xi}{1+\xi} \right) \cdot e^{-\frac{\pi}{(1+\xi) \cdot tg\left( \frac{\pi}{2} \cdot \frac{1-\xi}{1+\xi} \right)}} + \cos\left( \frac{\pi}{2} \cdot \frac{1-\xi}{1+\xi} \right) \right\}} \tag{39}$$

$$w_e = 0.882 \cdot \psi_{lab} \cdot \sqrt[3]{\frac{q_T^4}{D_K^2 \cdot \lambda \cdot c_e}} \tag{40}$$

Theoretical models are aimed at obtaining a possibly most precise representation of observed phenomena. Nevertheless, such models are only an approximation of real conditions. Figure 6 shows the relationship between the total resistance to motion of an idler set in various operating conditions and the conveyor's mass capacity

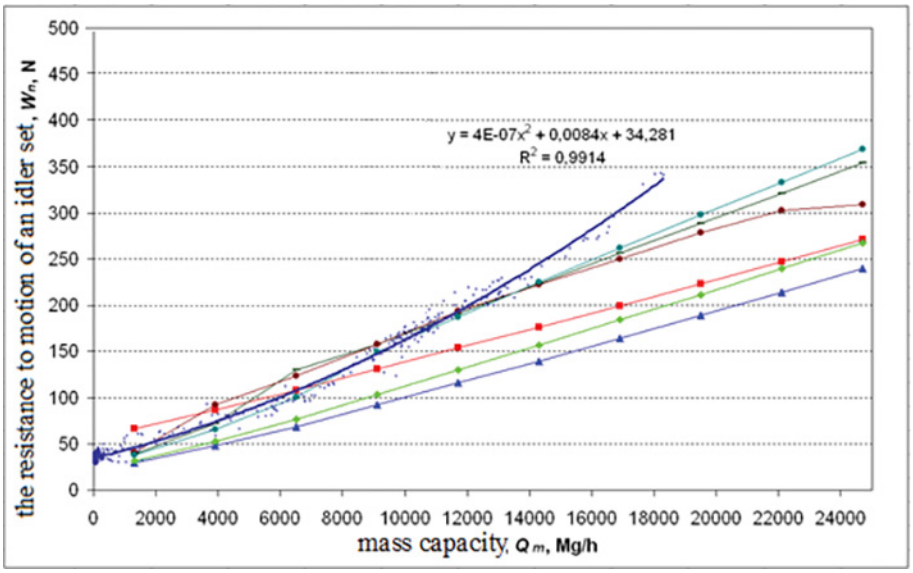


**Fig. 6.** Relationship between the resistance to motion of an idler set to mass capacity [12].

In the mass capacity range of 1000-12000 $\frac{Mg}{h}$, the resistances calculated for different variants are similar to the measurement results (dark blue line). As the capacity increases, however, the difference between the real values of motion resistances and the theoretical values becomes significant.

Although the above diagram has been plotted for total motion resistances, rolling resistances are notably the most significant component of main resistances. Rolling resistances may therefore, despite a number of additional elements, determine the motion resistance values of the whole conveyor. The diagram in Fig. 4 has been plotted on the basis of the previous theoretical model (5). Had the diagram been based on the assumptions for the new model, the actual, higher values of resistances would have been represented with greater precision.

## 6 Conclusions

The rolling resistances of the belt on idlers must be analyzed with regard to parameters which accommodate belt properties. In the analytical method, these properties are represented by damping factor and elastic modulus during cyclical compressing. Importantly, these parameters should be determinable in laboratory conditions. The hysteresis loops which are obtained in laboratory tests do not fully correspond to the loops obtained during cyclic indentation processes which occur on actual conveyors operated in mining conditions. The method described in this paper enables converting the damping factor calculated in laboratory tests into values which correspond to the actual operating conditions of a belt conveyor. Moreover, the share of rolling resistances in total motion resistances (for belt conveyors longer than 80 m) has been proven to be greater than previously believed. The new analytical model allows significantly more precise estimations of the resistances occurring on a belt conveyor.

Financial support by the project: Research, diagnostics and optimization of conveyor belt systems No. 0401/0166/16 and Grant no. 0401/0128/17.

## References

1. R. Król, W. Kisielewski, Mining Science – Fundamental Problems of Conveyor Transport, Vol. **21**(2) 61−72, Prague (2014)
2. R. Król, WMESS, 11-15 September (2017)
3. M. Bajda, R. Król, Procedia: Earth and Planetary Science, World Multidisciplinary Earth Sciences Symposium WMESS, Vol. **15**, 702-711 (2015)
4. L. Gładysiewicz, M. Konieczna, Mining Science, **Vol. 23**, 105-119 Wrocław (2016)
5. C.O. Jonkers, Forden und Haben, Vol. **30** No. 4 (1980)
6. G. Lodewijks, Bulk Solids Handling **23**(6), 384-391 (2003)
7. L. Gładysiewicz, *Przenośniki taśmowe Teoria i obliczenia,* Oficyna Wydawnictwo Politechniki Wrocławskiej, Wrocław (2003)
8. M. Hardygóra, M. Bajda, L. Gładysiewicz, Transport Przemysłowy, **3** (2007)
9. S. Drenkelford, *Energy-saving potential of Aramid-based conveyor belts*, Delft University of Technology (2015)
10. L. Gładysiewicz, Prace Naukowe CPBP 02.05. Wyd. Politechniki Warszawskiej, Warszawa (1990)
11. L. Gładysiewicz., M. Konieczna, Transport przemysłowy i maszyny robocze, **3** (2017)
12. W. Kisielewski, *Wpływ wybranych parametrów eksploatacyjnych i konstrukcyjnych na opory główne przenośników taśmowych*, PhD Thesis (not published), Wrocław University of Science and Technology (2016)